Received: 13 November 2019 | Revised: 11 March 2020 | Accepted: 21 April 2020
DOI: 10.1002/joc.6615

RESEARCH ARTICLE

International Journal of Climatology RMetS

# Tropical cyclone precipitation regimes since 1750 and the Great Suppression of 1843–1876 along coastal North Carolina, USA

**Paul A. Knapp**[1] | **Peter T. Soulé**[2] | **Justin T. Maxwell**[3] | **Jason T. Ortegren**[4] | **Tyler J. Mitchell**[1]

[1]Carolina Tree-Ring Science Laboratory, Department of Geography, Environment, and Sustainability, University of North Carolina Greensboro, Greensboro, North Carolina

[2]Appalachian Tree-Ring Laboratory, Department of Geography and Planning, Appalachian State University, Boone, North Carolina

[3]Environmental Tree-Ring Laboratory, Department of Geography, Indiana University, Bloomington, Indiana

[4]Department of Earth and Environmental Sciences, University of West Florida, Pensacola, Florida

**Correspondence**
Paul A. Knapp, Carolina Tree-Ring Science Laboratory, Department of Geography, Environment, and Sustainability, University of North Carolina Greensboro, Greensboro, NC.
Email: paknapp@uncg.edu

**Funding information**
NSF, Grant/Award Number: 1660432

**Abstract**
Latewood ring widths of longleaf pine (*Pinus palustris* Mill.) are effective recorders of annual variability of tropical cyclone (TC) precipitation (TCP), accounting for approximately half of the explained variance. Based on a regional chronology comprised of data from five sites in coastal North Carolina, we reconstructed TCP during 1750–2015 to examine temporal variability of multidecadal dry and wet TCP regimes, the synoptic controls that contributed to an exceptionally dry phase in 1843–1876, and the effectiveness of using latewood to identify droughts independent of TCP. We found six phases of alternating dry/wet phases occurred during the 250+ years in the reconstruction (duration range = 17–62 years) and the 1843–1876 period of exceptionally narrow latewood widths and low TCP values (i.e., the Great Suppression) was unique during the past quarter millennium. The Great Suppression coincided with a period of anomalously low pressure (relative mean hPa deviation = −60 DAM) over the eastern USA at 500 hPa heights, which strongly affects the steering of TCs. We found that while each dry phase was characterized by a persistence of these steering lows, including the most recent (2006–2016) period absent of major landfalling TCs in the United States, the Great Suppression was unmatched in intensity. Finally, we determined that variability in longleaf pine latewood widths do not reflect overall soil-moisture conditions, as neither narrow nor wide latewood widths are coincident with variations in non-TC-related precipitation. Rather, latewood growth flushes are associated with ephemeral periods of elevated water tables following high-intensity TC-related rainfall events.

**KEYWORDS**
dendroclimatology, longleaf pine, North Carolina, tropical cyclones, USA

## 1 | INTRODUCTION

Extreme rainfall totals associated with land-falling tropical cyclones (TCs) in the United States can cause billion-dollar disasters as observed with Hurricanes Harvey (2017, \$130), and Florence (2018, \$24.2) (NOAA, 2019). Heavy rainfall associated with these events has been attributed to a combination of enhanced atmospheric moisture (i.e., saturation specific humidity), increased abrupt directional deviations, and reduced translation speed as a function of the Earth's warming atmosphere (Kossin, 2018; Patricola and Wehner, 2018; Hall and Kossin, 2019). Thus, slow-moving systems with more meandering tracks are more likely to stall and combined with passage through a more humid atmosphere are more likely to produce copious amounts of precipitation (Hall and Kossin, 2019). Conversely, distinct periods absent major landfalling tropical cyclones in the United States also have occurred (Hall and Hereid, 2015), most recently during 2006–2016. Despite increasing evidence attributing higher TC rainfall totals to anthropogenic warming (e.g., van Oldenborgh *et al*., 2017; Wang *et al*., 2018), the inherent natural variability of TCs and brevity of spatially consistent historic records (Patricola and Wehner, 2018) complicates the understanding of the effects of anthropogenic warming. Thus, the inclusion of proxy tropical cyclone precipitation (TCP) data inferred from interannual variability of tree-ring widths formed during the TC season may help to place recent changes in a broader historical context.

Longleaf pine (*Pinus palustris* Mill.) latewood growth is significantly correlated with summer rainfall totals (e.g., Henderson and Grissino-Mayer, 2009; Patterson *et al*., 2016; Mitchell *et al*., 2019a) with the strongest relationships associated with slow-moving systems (i.e, stationary fronts, TCs) that produce 'soaker' rainfalls (e.g., Knapp *et al*., 2016; Mitchell *et al*., 2019b). On the coastal plains of North Carolina, TCP can account for 50% of the interannual variance of latewood ring widths (Knapp *et al*., 2016). In a study from two Carolina bay rim sites in North Carolina, Knapp *et al*. (2016) posited that the strong relationship between TCP and latewood ring widths was caused by elevated water tables post-TCP events that reached the extensive (up to 40 m diameter), yet shallow (depth < 0.3 m) lateral root systems of longleaf pine (Heyward, 1933). A follow-up study by Montpellier et al. (In Press) used high-resolution LiDAR data to measure elevations of longleaf pine on a sand rim at one of the Knapp *et al*. (2016) sites (Catfish Lake) and found a positive and significant ($p < .05$) relationship between rim elevation and latewood widths with TCP. Thus, their results support the hypothesis that longleaf pine growing on the higher portions of the rim are more responsive to TCP than those growing closer to the rim periphery. A consequence of this relationship between TCP and latewood growth, the latter of which occurs principally from June–mid-October and coincides with the core of the tropical cyclone season, is that latewood ring widths serve as proxies for TC rainfall totals.

Prior to extensive anthropogenic activity in the 18th and 19th centuries, including domestic livestock grazing, logging, naval stores extraction, and fire suppression (Frost, 2007), longleaf pine was the dominant tree species growing along the coastal plains of North Carolina. Covering approximately 70% of the landscape (Michaux, 1805 [1966]), the species is recognized for prodigious oleoresin production, from which naval stores including turpentine, tar, rosin, and pine oil were derived, and for the windfirm boles that were used for ship masts. Approximately 2.2% of the original range of longleaf pine remains intact, from the Delmarva Peninsula of northern Virginia to eastern Texas (Frost, 2007). In North Carolina, remnant stands along the Coastal Plain are principally limited to sites either too small or remote to harvest, including small pockets (0.02–0.05 $km^2$) of upland xeric old-growth stands on Carolina bay sand rims that rise 0.5–1.5 m above the surrounding pocosin bogs. At these sites, old-growth trees occur in stands with 20–50% crown cover and with several cohort age groups located in the canopy gaps (USDA, 2002).

Our prior work (Knapp *et al*., 2016) reconstructed TCP using longleaf pine data collected from two sites separated by 28 km on the central North Carolina coast during 1836–2014. We identified considerable interdecadal variability in latewood growth including a period of consistently narrow latewood bands during 1843–1876 (hereafter, the Great Suppression) that was unmatched during the 179-year record. However, we did not focus on the atmospheric steering mechanism(s) that would potentially explain multi-decadal phases of either above- or below-average TCP, whether there was a larger geographical signature to the wet/dry phases, or if the Great Suppression TCP amounts would remain unmatched using a near-century longer reconstruction period. Here, we use an expanded regional chronology based on combining updated tree-ring data from Knapp *et al*. (2016) with longleaf pine chronologies developed from three new sites in southeastern North Carolina to reconstruct TCP to 1750. Based on the new data analyses, we address three additional questions: (a) what does the reconstructed TCP record reveal about extended temporal regimes and regime shifts during the past 266-year period?; (b) what atmospheric forcing mechanisms were the likely driving forces for the Great Suppression?; and, (c) are narrow latewood bands indicative of deficits in total rainfall during the warm season or are they caused by a lack of TCP?

## 2 | METHODS

### 2.1 | Study area and tree-ring data

We collected tree-ring data at five sites in coastal North Carolina (Figure 1), the region that receives the most TCP in the United States both as an absolute and percentage of annual precipitation (Knight and Davis, 2007; Nogueira

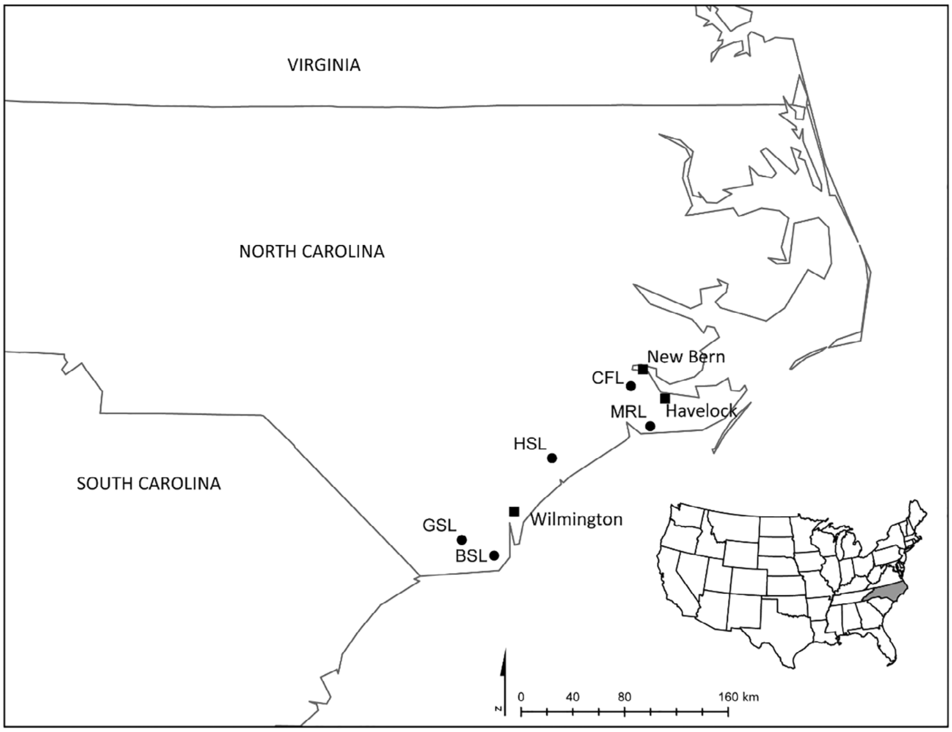


**FIGURE 1** Location of five tree-ring data collection sites (circles) and three climate stations (squares)

and Keim, 2011; Bregy *et al.*, 2020). We obtained all longleaf pine samples from trees located on sandy Carolina Bay rims. The rims, classified as wet pine flatwoods (Schafale, 2012), support longleaf pine woodlands with a wiregrass (*Aristida stricta* Michx.) understory prone to periodic (i.e., every 1–2 years) low-intensity fires (Frost 1996). At most sites, we saw minimal evidence of either naval stores activity (i.e., box cuts, chevrons) or logging, and potentially disturbed trees were not sampled. Furthermore, we saw no evidence of anthropogenic disturbance at study site HSL, which likely was unaffected because of difficult accessibility. Soil profiles (NRCS, 2019) for each site show either a sand or a fine-sand profile from 0 to 203 cm depth, slopes <2% and a water table depth of 0–30 cm. At each site, we obtained two core samples from 20 to 30 trees by sampling from the opposite sides of the tree at approximately 1-m height using increment borers. We selected only trees absent visible health issues (i.e., scars, disease, missing crowns, excessive needle damage) and growing in open-canopy conditions. For each tree, we measured DBH, canopy height, and geographic coordinates. We collected all our samples during 2012–2018. Additionally, at each site, we obtained 5–15 cross-sections from remnant stumps to extend the chronology. Because the common period of our five-site regional representation was only complete through 2015, we ended our analyses at 2015.

We processed all samples following standard dendrochronological methods (Stokes and Smiley, 1968; Phipps, 1985; Swetnam *et al.*, 1985; Speer, 2010). We first glued the live-tree samples onto wood mounts, sanded using 120–600 *u*m grit to reveal cellular structure and cross-dated with the list method (Yamaguchi, 1991). We used Windendro (Version 2017a) to measure earlywood, latewood, and total ring widths and then verified cross-dating accuracy using COFECHA (Holmes, 1983) with adjustments made to correct dating errors. We standardized the final latewood North Carolina regional chronology (hereafter NCR), which represented the combination of the five sites ($n$ = 164 cores), using the negative exponential curve option in ARSTAN (Cook, 1985) as the trees were in an open, woodland environment without canopy overlap. We obtained mean values for interseries correlation and subsample signal strength (Holmes, 1983; Cook, 1985) from the COFECHA and ARSTAN outputs. Additionally, because single-year values of the NCR chronology ranged from .27 to >2.59 with a mean of 0.72, we subsequently converted these values into z-scores to help in the interpretation of latewood growth deviations.

## 2.2 | Climate data and tropical cyclone precipitation reconstruction

We obtained precipitation totals attributed to tropical cyclone events from the three stations nearest the tree-ring data-collection sites during 1953–2015 using either complete (Wilmington: USW00013748) or nearly complete daily records (New Bern: USW00093719 and Havelock: USW00013754) (Figure 1). We replaced missing data for Havelock (1999–2000) with data from New Bern

(1994–1997) and vice versa as these stations were at the same elevation and separated by approximately 28 km. For each station, we used IBTrACS; (Knapp *et al.*, 2010) to record precipitation that occurred on days when TCs tracked through a 223 km-radius rain field (Matyas, 2010; Zhou and Matyas, 2017) centred over each station during June first–October 15, which is the period that has the strongest association with latewood growth (Knapp *et al.*, 2016). We matched TCs that tracked through the rain field at 6z, 12z, 18z, and next-day 0z with current-day precipitation. Our method is designed to isolate TCP amounts and is comparable to what other studies (e.g., Knight and Davis, 2007; Bregy *et al.*, 2020) have employed. That said, it is not possible to fully isolate TCP from other rainfall sources (e.g., convective or frontal) on the day(s) TCs tracked through the study area and non-TCP rainfall may be included on some days.

We used a linear regression model to reconstruct TCP from 1750–2015 using 1953–2015 as the calibration period. We used TCP data as the dependent variable and the NCR chronology as the independent variable. To determine if the relationship between TCP and the NCR chronology was temporally stable, we used a standard split-period validation procedure. First, we calibrated the model using the early period (1953–1983) and verified for the later period (1984–2015) using R package treeclim (Zang and Biondi, 2015). We reversed the process by calibrating the model on the 1984–2015 period and then verified on the early period. Specifically, we used reduction of error (RE) and coefficient of efficiency statistics (CE) as validation statistics for both calibration and verification periods.

### 2.3 | Regime shift analysis and climate anomaly mapping

We identified regime shifts in standardized latewood radial growth and reconstructed TCP during 1750–2015 using the Regime Shift Analysis (RSA) program ver. 3.2 by Rodionov (2006), an alpha of 0.05, a cut-off length of 10 years, and a Huber's weight parameter of 1. Cut-off lengths represent a minimum period in which all regimes longer than the length are recorded, with the reduced probability of regime shift detection for shorter periods. Huber weights are parameters that determine the influence of outliers with each whole number representing a standard deviation and the number representing equal weighting for values with standard deviations less than or equal to the number selected. RSA produces time periods (i.e., regimes) with means that are significantly different from adjacent regimes but does not make statistical distinctions between non-adjacent phases. Thus, we used one-way analysis of variance (ANOVA) with Tukey HSD tests (SPSS ver. 22) to determine if regimes of either latewood or reconstructed TCP were significantly ($p < .05$) different beginning with the first full regime (1764–1780). Two incomplete regime shifts 1750–1763 and 2015 were not included for analysis as either their beginning or ending dates were unknown. As the TCP reconstruction is derived from the standardized latewood widths, we recognize that regimes identified for both are identical. However, we present both, as the means of TCP and latewood width associated with specific regimes are illustrative.

We examined climate proxies to determine if they would support our reconstructed TCP data. We evaluated upper-level atmospheric conditions during 1851–2014 using 20th Century Reanalysis V2 data provided by the NOAA/OAR/ESRL PSD (https://www.esrl.noaa.gov/psd/). We mapped mean 500 hPa height anomalies during June–September over the region $0^\circ$–$60^\circ$N and $0^\circ$–$130^\circ$ W to assess conditions that prevailed during: (a) complete TCP phases as defined by RSA; and, (b) the 10 driest and wettest reconstructed TCP years that coincided with the Reanalysis V2 data. In addition, we used IBTrACS data to identify the frequency (i.e., number of TCs) and duration (i.e., number of 6-hour segments) of TCs that tracked through our study region during 1851–2015 with the 223 km-radius centre located over HSL, the approximate midpoint between the northernmost and southernmost stations. To expand the TC frequency and duration record to 1843, which begins a 34-year period of suppressed growth, we examined records identified by Barnes (2013), who used newspaper reports, historical documents, letters, and oral histories to identify the date and locations affected by tropical cyclones. For years with no storms recorded, we entered zeros for both frequency and duration. Conversely, possible TC activity occurred in 1846 and 1850 and those years were treated as missing data as we could not determine either exact storm tracks or duration.

## 3 | RESULTS

### 3.1 | Tree-ring statistics, calibration and verification, and climate data

The NCR chronology spanned from 1695 to 2018 and consists of 164 cores with a subsample signal strength of 0.80 beginning in 1750. The interseries correlation is 0.50, comparable to other studies (e.g., Henderson and Grissino-Mayer, 2009; Knapp *et al.*, 2016) that have used longleaf pine latewood on the Atlantic coastal plains. The 1750–2015 TCP reconstruction model

**TABLE 1** Grouping of reconstructed TCP regimes by mean values (mm)

| RSA phase | Regime length (years) | Regime groupings by TCP 1 = driest, 4 = wettest 1 | 2 | 3 | 4 |
|---|---|---|---|---|---|
| 1764–1780 | 17 | | | 111.7 | 111.7 |
| 1781–1842 | 62 | | 83.4 | 83.4 | |
| 1843–1876 | 34 | 17.6 | | | |
| 1877–1932 | 56 | | 65.8 | | |
| 1933–1964 | 32 | | | | 127.8 |
| 1965–2014 | 50 | | 58 | | |

*Note*: Multiple values within a group (i.e., column) indicate the regime is not significantly different (alpha > 0.05) from other group entries based on ANOVA with Tukey HSD test.

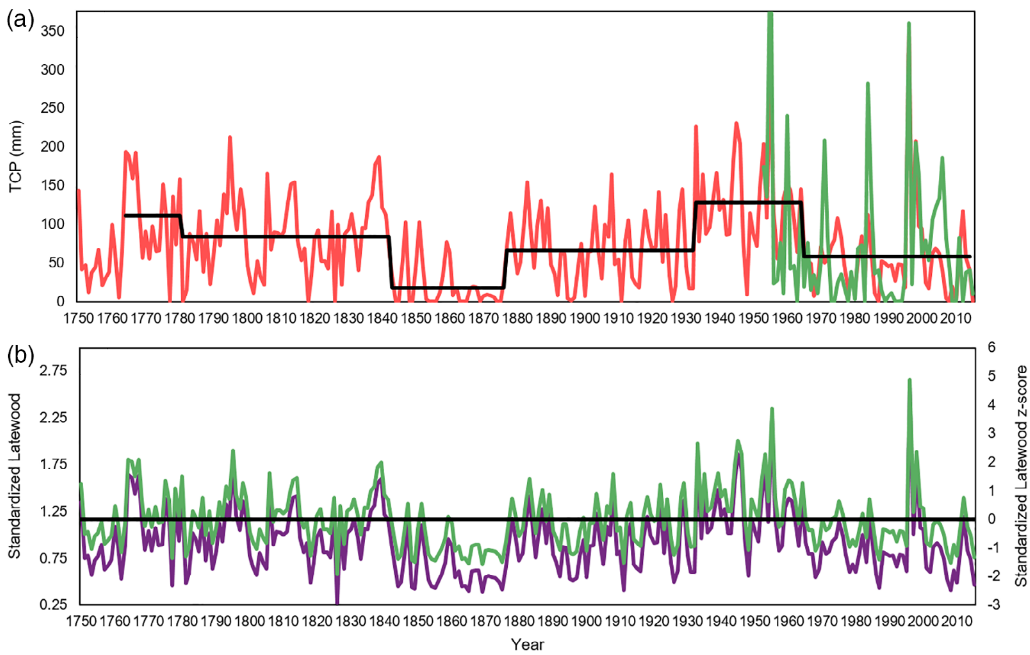


**FIGURE 2** (a) Reconstructed TCP (mm) during 1750–2015 with actual TCP during 1953–2015. Reconstructed TCP values <0 are shown as 0. Mean values of RSA phases of reconstructed TCP (multidecadal flat-line segments) are listed in Table 1. (b) Standardized latewood (lower line) and Z-scores of standardized latewood (upper line) during 1750–2015 with z-score mean (flat line) [Colour figure can be viewed at wileyonlinelibrary.com]

explained 50.4% of observed TCP variance during 1953–2015. Split-period validation statistics were positive for both the early (1953–1983) and late periods (1984–2015), with RE values of .32 (early) and .45 (late) and CE values of .32 (early) and .45 (late). Values >0 indicate the model sufficiently incorporated observed variance necessary for reconstruction (Cook *et al.*, 1994; Fritts, 2012). Mean reconstructed TCP (71.2 mm·year$^{-1}$) matched actual mean TCP (72.2 mm·year$^{-1}$) during the historic period (1953–2015) and represented 10.3% of all precipitation ($\bar{x}$ = 689.1 mm) during June 1– October 15 and 5.2% of annual precipitation ($\bar{x}$ = 1,373.6 mm). Non-TCP (i.e., rainfall total during June 1–October 15, excluding TCP) was not significantly correlated with reconstructed TCP ($r = 0.008$, $p = 0.953$) during 1953–2015.

## 3.2 | Regime shifts and climate anomaly mapping

RSA identified six complete TCP regime shifts with durations ranging from 17–62 years (Table 1, Figure 2a). The driest period of TCP ($\bar{x}$ = 17.6 mm) occurred during 1843–1876 ($n = 34$ years) and was the only period significantly ($p < .01$) different from the five other phases. The

**TABLE 2** Grouping of standardized latewood (latewood z) regimes

| RSA phase | Regime length (years) | Regime groupings by latewood (latewood Z) 1 = narrowest, 4 = widest | | | |
|---|---|---|---|---|---|
| | | 1 | 2 | 3 | 4 |
| 1764–1780 | 17 | | | 1.16 (.69) | 1.16 (.69) |
| 1781–1842 | 62 | | 1 (.20) | 1 (.20) | |
| 1843–1876 | 34 | .61 (−.93) | | | |
| 1877–1932 | 56 | | 0.89 (−0.1) | | |
| 1933–1964 | 32 | | | | 1.26 (.97) |
| 1965–2014 | 50 | | 0.85 (−.23) | | |

*Note*: Multiple values within a group (i.e., column) indicate the regime is not significantly different (alpha > 0.05) from other group entries based on ANOVA with Tukey HSD test.

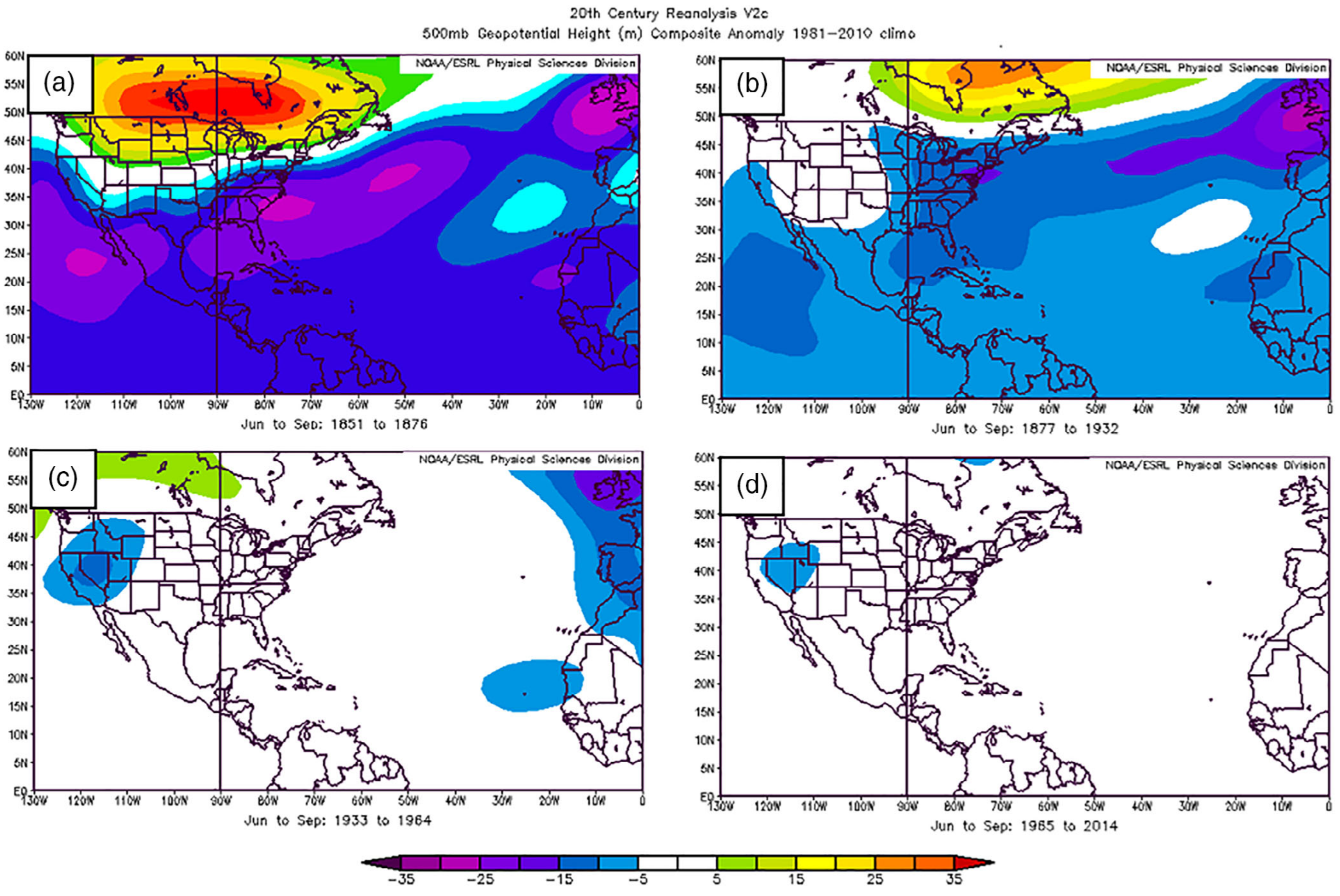


**FIGURE 3** The mean 500 hPa height anomalies during TCP phases of 1851–2014: (a) 1843–1876, (b) 1877–1932, (c) 1933–1964, and (d) 1965–2014. The 1843–1876 phase is truncated by lack of data prior to 1851 [Colour figure can be viewed at wileyonlinelibrary.com]

wettest phase occurred during 1933–1964 ($\bar{x}$ =127.8 mm). No long-term trend ($R^2$ =0.00, $p$ =.79) in reconstructed TCP occurred during 1750–2015 (Figure 2a). During 1843–1876, mean reconstructed TCP was 24.6% of the reconstructed mean and 30.3% of the next-driest phase of 1965–2014. Conversely, reconstructed TCP during 1933–1964 represented 178.9% of the reconstructed average, but was only 14.4% wetter than the second-wettest phase of 1764–1780. Latewood z-scores during the driest (wettest) phase were both approximately one SD below (above) the mean (Figure 2a, Table 2). However, the phases were represented differently, with the driest phase marked by consistently narrow latewood with 20 of 34 years having z-scores <−1. Comparatively,

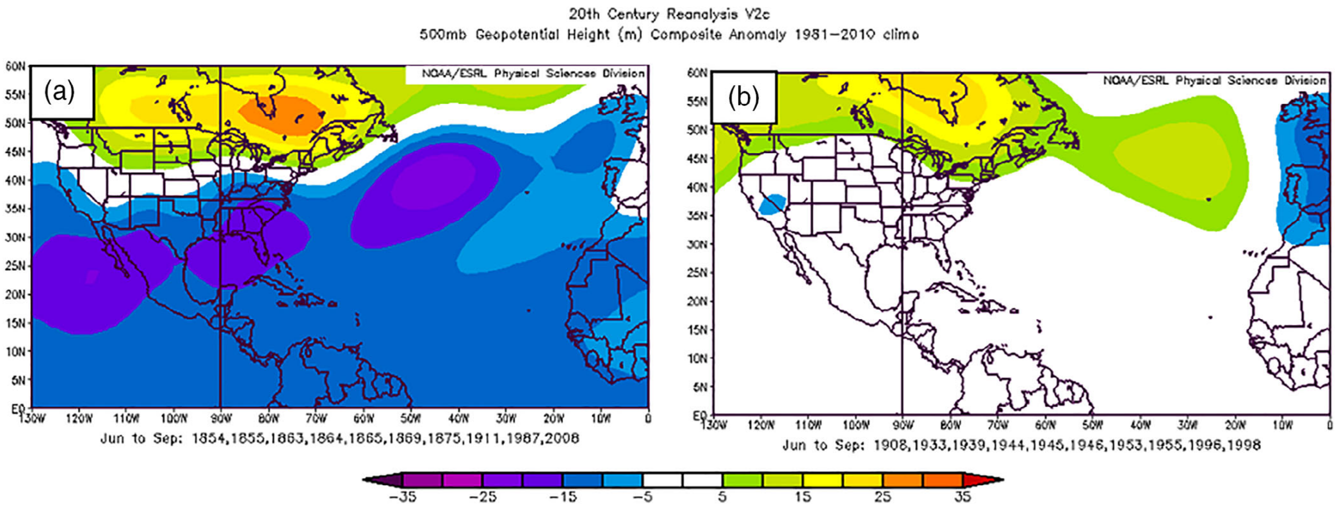


**FIGURE 4** The mean 500 hPa height anomalies during: (a) the 10 driest and (b) the 10 wettest reconstructed TCP years during 1851–2015 [Colour figure can be viewed at wileyonlinelibrary.com]

the 1933–1964 wet phase was less consistent, with 14 of 32 years with z-scores >1 (Figure 2b).

During 1851–2014, 500 hPa height anomalies show distinct patterns during the four regimes identified by RSA (Figure 3a–d) as well as the 10 driest (wettest) years of TCP (Figure 4a,b). The 1843–1876 low TCP regime was marked by ridging over the southern Canadian Great Plains and troughing both in the North Atlantic centred at (40, −50) and in the southeastern USA (Figure 3a). The wettest phase of 1933–1964 was marked by the absence of 500 hPa height anomalies in eastern North America and the North Atlantic (Figure 3c). Examination of the 10 driest years based on reconstructed TCP also shows a similar, but exaggerated 500 hPa pattern compared to the 1843–1876 dry phase (Figure 4a). Conversely, the 10 wettest years of reconstructed TCP are marked by a region of ridging in the North Atlantic approximately 15°E of the trough present during drier years (Figure 4b). Relationships between reconstructed TCP and both TC frequency ($r = .363$, $p < .01$) and duration ($r = .307$, $p < .01$) during 1843–2015 were significant, but modest.

## 4 | DISCUSSION

The six distinct TCP regimes that occurred during 1764–2014 suggest alternating dry/wet multidecadal phases extend beyond those documented using historic data to examine Atlantic tropical cyclone rainfall contributions (e.g., Cry, 1967; Knight and Davis, 2007; Nogueira and Keim, 2011). The duration of these historical studies ranged from 25 to 48 years covering the collective period of 1930–2007, but the study periods were not selected based on TCP regimes. That said, both Knight and Davis (2007) and Nogueira and Keim (2011) identified trends towards wetter/drier conditions that were associated with fluctuations in the Atlantic multidecadal oscillation (AMO), but did not examine the spatial patterns of upper-atmospheric conditions that would work as steering mechanisms affecting tracking of TCs. Our results suggest that distinctive patterns of upper-level pressure anomalies (i.e., 500 hPa) occur during both multidecadal phases (Figure 3) and extreme dry or wet years (Figure 4), but that the greatest anomalies occur during dry phases and years.

The most exceptional dry phase since 1750 occurred during 1843–1876 (Great Suppression) and is the only phase that is significantly different from all others. During this 34-year period, TCP averaged <25% of the 267-year mean of 71.6 mm. In comparison, the next driest phase of 1965–2014 averaged 81% of the long-term average. The Great Suppression dry phase is unlikely an artifact of human impact (i.e., naval stores activity) on the sampled trees. We purposely avoided sampling longleaf pine with scarring from turpentining activities and the narrow growth rings were present from trees cored at HSL, which is a site surrounded by wetlands thus too inaccessible to commercially utilize. Furthermore, our results of low TCP amounts are consistent with reduced TC frequency and duration during our study period.

The mean 500 hPa pattern during the Great Suppression is marked by consistent troughing along the southeastern U.S. coastline, centred over the Carolinas and extending to the central North Atlantic, and a ridge east of Hudson Bay, Canada (Figure 2a). This pattern is repeated when examining the 10-driest years since 1843

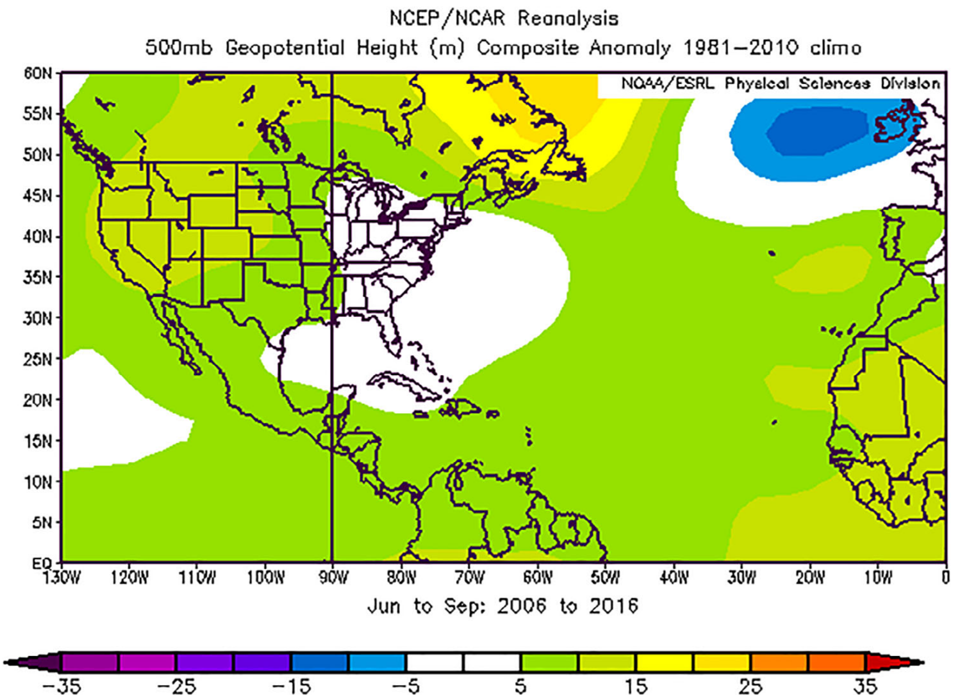


**FIGURE 5** The mean 500 hPa height anomalies during 2006–2016 when no major hurricane made landfall in the United States [Colour figure can be viewed at wileyonlinelibrary.com]

(Figure 4a), suggesting a consistency in the conditions that promote dry years or phases. The negative anomalies at 500 hPa along the southeastern U.S. coast would produce winds that would steer tropical cyclones northeastward and away from the Carolinas, thus, working as steering lows.

We also examined atmospheric conditions present during the most recent period (2006–2016) of reduced landfalling tropical cyclone activity along the East Coast of the U.S. (Hall and Hereid, 2015). During this 11-year period, our mean reconstructed TCP was 31.6 mm (44% of the multi-century mean), indicating that below-average TCP was coincident with an absence of landfalling major hurricanes (i.e., 'hurricane droughts', Hall and Hereid, 2015, p. 3482). Similarly, Truchelut and Staehling (2017) found that accumulated cyclone energy values for the Atlantic Basin during the 2006–2016 period absent of hurricanes were unprecedented during the period of reliable records (1950–2017). Likewise, the 500 hPa patterns during 2006–2016 (Figure 5) are consistent with the presence of troughing along the eastern U.S. coastline (relative to the surrounding regions), but the extent of the low is less pronounced than during the Great Suppression. Relative differences in 500 hPa heights between the ridge east of Hudson Bay and troughing over the east coast were approximately −60 DAM during the Great Suppression and −20 DAM during the modern hurricane drought (Figures 3a and 4).

Our results do not address the extent of TC activity in the Atlantic Basin but rather the phases marked by either below- or above-average TC landfall (or near landfall) activity that would affect TCP totals. Several (e.g., Klotzbach *et al.*, 2015; Staehling and Truchelut, 2016; Truchelut and Staehling, 2017; Kossin, 2018) have found that during active Atlantic Basin TC seasons, conditions near the coast may decrease the likelihood of TC landfall. In particular, the presence of deep troughing along the eastern U.S. coast (Klotzbach and McNoldy, 2015) may serve as a 'hurricane goalkeeper' (Mooney, 2017) preventing TCs from making landfall and consistent with the pattern present during the Great Suppression.

The cause(s) promoting the anomalously low 500 hPa heights during the Great Suppression remain unclear. The frequency of landfalling TCs in the southeastern U.S. is principally affected by both ENSO conditions and AMO phases (Klotzbach *et al.*, 2018). There is a significantly higher frequency of landfalling TCs during La Niña seasons compared to El Niño seasons (1.4 vs 0.8 landfalls year$^{-1}$), but this relationship is less extreme regarding major TCs (0.4 vs. 0.1). Likewise, positive AMO conditions are significantly associated with more landfalling TCs and with higher total rainfall from TCs (Nogueira and Keim, 2011) than negative AMO conditions (1.3 vs. 0.8), but the association is less pronounced (0.4 vs. 0.2) for major hurricanes (Klotzbach *et al.*, 2018). The AMO positive/negative phases identified by Klotzbach and Gray (2008) do not match the phase shifts we identified using RSA, and ENSO variability tends to cycle at higher frequencies (~2–7 years) than the reconstructed multidecadal phases of TCP, suggesting other cause(s) were operative (Cordery and McCall, 2000). Furthermore, the impact of volcanic aerosols has been cited as a cause of reduced TC activity in the North Atlantic, particularly within 3 years post-eruption (e.g., Guevara-Murua *et al.*, 2015). However, the onset of phase shifts did not coincide with major eruptive events (identified as years with >0.02 Sulfate Aerosol Optical Depth [SAOD] values), nor did the phases correspond with periods of lower or higher SAOD values (Crowley and Unterman, 2013). Our results are consistent with Camargo and Polvani (2019) who found insufficient evidence supporting reduced TC activity post-eruption.

Despite the strong affinity of latewood growth with TCP that accounts for 50.4% of the interannual variance, non-TCP rainfall totals during June 1–October 15 are not significantly ($p < .05$) associated with variations for either latewood growth or TCP. These results suggest independence between synoptic controls associated with TCP and non-TCP precipitation and thus, narrow latewood ring widths obtained from longleaf pine within coastal Carolina should not be used to infer droughts within the region as the TCP contribution represents approximately a 10th of the total summertime rainfall. For example, four of the 10 wettest summers (i.e., combined TCP and non-TCP values) during 1953–2015 occurred in years with below-average TCP totals. Conversely, while low TCP totals are not a cause of droughts, major TCP events are climatologically important in the context that major TCP events can end droughts (e.g., Maxwell *et al.*, 2012, 2013).

## 5 | CONCLUSIONS

Latewood bands of longleaf pine effectively record TCP and can be used to identify multidecadal periods of above- and below-average TCP. Of the six phases we identified during the past quarter millennium, the dry phase of 1843–1876 was unmatched in extent, suggesting a substantial reduction in TC activity. Coincident with the Great Suppression and other phases of reduced TCP were anomalously low 500 hPa pressure heights along the southeastern U.S. coastline. This pattern is indicative of persistence in steering lows that effectively blocked TCs from making landfall and steered them towards the northeast and away from land. Our results reveal that more extreme periods of reduced landfalling TC activity have likely occurred when compared to the most recent period of 2006–2016. Finally, TCP is ecologically important to longleaf pine and is an effective mechanism to end droughts abruptly. However, we found TCP variability to work independently of non-TCP events and thus the use of longleaf pine latewood bands to assess drought may not be optimal.

## ACKNOWLEDGEMENTS

Research was supported by funding from NSF Grant GSS-1660432. We thank the field/lab assistants that made this project possible: Tsun Fung Au, Josh Bregy, April Kaiser, Andrew Matej, Tyler Mitchell, Evan Montpellier, Thomas Patterson, Brandon Strange, and Jeffy Summers. We are grateful for the help of Andrew Walker of the Croatan National Forest Service office who helped us in accessing field sites and offered insights on longleaf pine ecological processes.

## ORCID

*Paul A. Knapp* https://orcid.org/0000-0002-0783-7933

## REFERENCES

Barnes, J. (2013) *North Carolina's Hurricane History*. Chapel Hill, NC: University of North Carolina Press.

Bregy, J.C., Maxwell, J.T., Robeson, S.M., Ortegren, J.T., Soulé, P.T. and Knapp, P.A. (2020) Spatiotemporal variability of tropical cyclone precipitation using a high-resolution, gridded (0.25 x 0.25) dataset for the eastern United States, 1948–2015. *Journal of Climate*, 33(5), 1803–1819.

Camargo, S.J. and Polvani, L.M. (2019) Little evidence of reduced global tropical cyclone activity following recent volcanic eruptions. *npj Climate and Atmospheric Science*, 2(1), 14. https://doi.org/10.1038/s41612-019-0070-z.

Cook, E.R. (1985) *A Time Series Analysis Approach to Tree Ring Standardization*. Dissertation: University of Arizona.

Cook, E.R., Briffa, K.R. and Jones, P.D. (1994) Spatial regression methods in dendroclimatology: a review and comparison of two techniques. *International Journal of Climatology*, 14(4), 379–402.

Cordery, I. and McCall, M. (2000) A model for forecasting drought from teleconnections. *Water Resources Research*, 36(3), 763–768. https://doi.org/10.1029/1999WR900318.

Crowley, T.J. and Unterman, M.B. (2013) Technical details concerning development of a 1200 yr proxy index for global volcanism. *Earth System Science Data*, 5(1), 187–197. https://doi.org/10.5194/essd-5-187-2013.

Cry, G.W. (1967) *Effects of Tropical Cyclone Rainfall on the Distribution of Precipitation over the Eastern and Southern United States*. Washington: U.S. Department of Commerce, Environmental Science Services Administration.

Fritts, H. (1976) *Tree Rings and Climate*. London: Academic Press.

Frost C. 1996. Presettlement Vegetation and Natural Fire Regimes of the Croatan National Forest. Unpublished report, USDA Forest Service, Croatan National Forest, Asheville, NC.

Frost, C. (2007) History and future of the longleaf pine ecosystem. In: Jose, S., Jokela, E.J. and Miller, D.L. (Eds.) *The Longleaf Pine Ecosystem. Springer Series on Environmental Management*. New York, NY: Springer, pp. 9–48.

Guevara-Murua, A., Hendy, E.J., Rust, A.C. and Cashman, K.V. (2015) Consistent decrease in North Atlantic tropical cyclone frequency following major volcanic eruptions in the last three centuries. *Geophysical Research Letters*, 42(21), 9425–9432. https://doi.org/10.1002/2015GL066154.

Hall, T. and Hereid, K. (2015) The frequency and duration of U.S. hurricane droughts. *Geophysical Research Letters*, 42(9), 3482–3485. https://doi.org/10.1002/2015GL063652.

Hall, T.M. and Kossin, J.P. (2019) Hurricane stalling along the north American coast and implications for rainfall. *npj Climate and Atmospheric Science*, 2(1), 17. https://doi.org/10.1038/s41612-019-0074-8.

Henderson, J.P. and Grissino-Mayer, H.D. (2009) Climate–tree growth relationships of longleaf pine (*Pinus palustris* mill.) in the southeastern coastal plain, USA. *Dendrochronologia*, 27(1), 31–43.

Heyward, F. (1933) The root system of longleaf pine on the Deep Sands of Western Florida. *Ecology*, 14(2), 136–148. https://doi.org/10.2307/1932880.

Holmes, R.L. (1983) Computer-assisted quality control in tree-ring dating and measurement. *Tree-Ring Bulletin*, 43, 69–78.

Klotzbach, P., Gray, W. and Fogarty, C. (2015) Active Atlantic hurricane era at its end? *Nature Geoscience*, 8(10), 737–738. https://doi.org/10.1038/ngeo2529.

Klotzbach PJ, McNoldy B. 2015. Recurring east coast low pressure may be saving U.S. from major hurricanes. The Washington Post, Capital Weather Gang. Available at: https://www.washingtonpost.com/news/capital-weather-gang/wp/2015/12/09/recurring-east-coast-low-pressure-may-be-saving-u-s-from-major-hurricanes/

Klotzbach, P.J., Bowen, S.G., Pielke, R. and Bell, M. (2018) Continental U.S. hurricane landfall frequency and associated damage: observations and future risks. *Bulletin of the American Meteorological Society*, 99(7), 1359–1376. https://doi.org/10.1175/BAMS-D-17-0184.1.

Klotzbach, P.J. and Gray, W.M. (2008) Multidecadal variability in North Atlantic tropical cyclone activity. *Journal of Climate*, 21 (15), 3929–3935. https://doi.org/10.1175/2008JCLI2162.1.

Knapp, K.R., Kruk, M.C., Levinson, D.H., Diamond, H.J. and Neumann, C.J. (2010) The international best track archive for climate stewardship (IBTrACS) unifying tropical cyclone data. *Bulletin of the American Meteorological Society*, 91(3), 363–376.

Knapp, P.A., Maxwell, J.T. and Soulé, P.T. (2016) Tropical cyclone rainfall variability in coastal North Carolina derived from longleaf pine (*Pinus palustris* Mill.): AD 1771–2014. *Climatic Change*, 135(2), 311–323. https://doi.org/10.1007/s10584-015-1560-6.

Knight, D.B. and Davis, R.E. (2007) Climatology of tropical cyclone rainfall in the southeastern United States. *Physical Geography*, 28(2), 126–147.

Kossin, J.P. (2018) A global slowdown of tropical-cyclone translation speed. *Nature*, 558(7708), 104–107. https://doi.org/10.1038/s41586-018-0158-3.

Matyas, C.J. (2010) Associations between the size of hurricane rain fields at landfall and their surrounding environments. *Meteorology and Atmospheric Physics*, 106(3–4), 135–148. https://doi.org/10.1007/s00703-009-0056-1.

Maxwell, J.T., Ortegren, J.T., Knapp, P.A. and Soulé, P.T. (2013) Tropical cyclones and drought amelioration in the Gulf and southeastern coastal United States. *Journal of Climate*, 26(21), 8440–8452. https://doi.org/10.1175/JCLI-D-12-00824.1.

Maxwell, J.T., Soulé, P.T., Ortegren, J.T. and Knapp, P.A. (2012) Drought-busting tropical cyclones in the southeastern Atlantic United States: 1950–2008. *Annals of the Association of American Geographers*, 102(2), 259–275. https://doi.org/10.1080/00045608.2011.596377.

Michaux, F.A. (1805 [1966]) *Travels to the West of the Alleghany Mountains*. Cleveland, Ohio: The Arthur H. Clark Company.

Mitchell, T.J., Patterson, T.W. and Knapp, P.A. (2019a) Comparison of climate–growth responses of montane and piedmont longleaf pine (*Pinus palustris* mill.) chronologies in North Carolina. *Trees*, 33, 615–620. https://doi.org/10.1007/s00468-019-01823-8.

Mitchell, T.J., Knapp, P.A. and Patterson, T.W. (2019b) Changes in southeastern USA summer precipitation event types using instrumental (1940–2018) and tree-ring (1790–2018) data. *Environmental Research Communications*, 1, 111005. https://doi.org/10.1088/2515-7620/ab4cd6.

Montpellier, E.E., Knapp, P.A., Soule', P.T., and Maxwell, J.T. (In Press) Microelevational differences affect longleaf pine (Pinus palustris Mill.) sensitivity to tropical cyclone precipitation: a case study using LiDAR. *Tree-Ring Research*.

Mooney C. 2017. The science behind the U.S.'s strange hurricane “drought”—and its sudden end. Capital Weather Gang September 7th. Available at: https://www.washingtonpost.com/news/energy-environment/wp/2017/09/07/the-science-behind-the-u-s-s-strange-hurricane-drought-and-its-sudden-end/.

NOAA, National Centers for environmental information (NCEI). 2019. U.S. Billion-Dollar Weather and Climate Disasters. Available at: https://www.ncdc.noaa.gov/billions/.

Nogueira, R.C. and Keim, B.D. (2011) Contributions of Atlantic tropical cyclones to monthly and seasonal rainfall in the eastern United States 1960–2007. *Theoretical and Applied Climatology*, 103(1–2), 213–227.

National Resources Conservation Service (NRCS). 2019. Web Soil Survey, North Carolina, USA. Available at: https://websoilsurvey.nrcs.usda.gov/app/WebSoilSurvey.aspx.

Patterson, T.W., Cumming, L.W. and Knapp, P.A. (2016) Longleaf pine (*Pinus palustris* mill.) morphology and climate/growth responses along a physiographic gradient in North Carolina. *The Professional Geographer*, 68(2), 238–248. https://doi.org/10.1080/00330124.2015.1059404.

Patricola, C.M. and Wehner, M.F. (2018) Anthropogenic influences on major tropical cyclone events. *Nature*, 563(7731), 339–346. https://doi.org/10.1038/s41586-018-0673-2.

Phipps, R.L. (1985) *Collecting, Preparing, Crossdating, and Measuring Tree Increment Cores*. Geological Survey: US Department of the Interior.

Rodionov, S.N. (2006) Use of prewhitening in climate regime shift detection. *Geophysical Research Letters*, 33(12), L12707. https://doi.org/10.1029/2006GL025904.

Schafale, M.P. (2012) *Classification of the Natural Communities of North Carolina: Fourth Approximation. North Carolina Department of Environment and Natural Resources*. Raleigh, NC: Natural Heritage Program.

Speer, J.H. (2010) *Fundamentals of Tree-Ring Research*. Tucson, AZ: University of Arizona Press.

Staehling, E.M. and Truchelut, R.E. (2016) Diagnosing United States hurricane landfall risk: an alternative to count-based methodologies. *Geophysical Research Letters*, 43(16), 8798–8805. https://doi.org/10.1002/2016GL070117.

Stokes, M. and Smiley, T. (1968) *An Introduction to Tree-Ring Dating*. Chicago Press, IL: University of Chicago.

Swetnam, T.W., Thompson, M.A. and Sutherland, E.K. (1985) *Using Dendrochronology to Measure Radial Growth of Defoliated Trees*. Forest Service, Cooperative State Research Service: US Department of Agriculture.

Truchelut, R.E. and Staehling, E.M. (2017) An energetic perspective on United States tropical cyclone landfall droughts: U.S. tropical cyclone landfall droughts. *Geophysical Research Letters*, 44(23), 12,013–12,019. https://doi.org/10.1002/2017GL076071.

van Oldenborgh, G.J., van der Wiel, K., Sebastian, A., Singh, R., Arrighi, J., Otto, F., Haustein, K., Li, S., Vecchi, G. and Cullen, H. (2017) Attribution of extreme rainfall from hurricane Harvey, August 2017. *Environmental Research Letters*, 12 (12), 124009. https://doi.org/10.1088/1748-9326/aa9ef2.

USDA. 2002. Croatan National Forest Land and Resource Management Plan. 142.

Wang, S.-Y.S., Zhao, L., Yoon, J.-H., Klotzbach, P. and Gillies, R. R. (2018) Quantitative attribution of climate effects on hurricane Harvey's extreme rainfall in Texas. *Environmental Research Letters*, 13(5), 054014. https://doi.org/10.1088/1748-9326/aabb85.

Yamaguchi, D.K. (1991) A simple method for cross-dating increment cores from living trees. *Canadian Journal of Forest Research*, 21(3), 414–416.

Zang, C. and Biondi, F. (2015) Treeclim: an R package for the numerical calibration of proxy-climate relationships. *Ecography*, 38, 431–436. https://doi.org/10.1111/ecog.01335.

Zhou, Y. and Matyas, C.J. (2017) Spatial characteristics of storm-total rainfall swaths associated with tropical cyclones over the eastern United States. *International Journal of Climatology*, 37, 557–569. https://doi.org/10.1002/joc.5021.

**How to cite this article:** Knapp PA, Soulé PT, Maxwell JT, Ortegren JT, Mitchell TJ. Tropical cyclone precipitation regimes since 1750 and the Great Suppression of 1843–1876 along coastal North Carolina, USA. *Int J Climatol*. 2020;1–11. https://doi.org/10.1002/joc.6615